Take a deep dive into the business of transplantation!

2021 Digital Kidney & Liver Transplant Financial Bootcamp

Self-paced: access at your convenience

Access Online!

Register at ASTS.org/bootcamps

ASTS
American Society of Transplant Surgeons®

ORIGINAL ARTICLE

Dominant regulation of long-term allograft survival is mediated by microRNA-142

Nelomi Anandagoda[1] | Luke B. Roberts[1] | Joanna C. D. Willis[1] |
Padmini Sarathchandra[2] | Fang Xiao[3] | Ian Jackson[1] | Arnulf Hertweck[4] |
Puja Kapoor[1] | Richard G. Jenner[4] | Jane K. Howard[3] | Graham M. Lord[1,5]

[1]School of Immunology and Microbial Sciences, King's College London, London, UK

[2]Heart Science Centre, Harefield Hospital, National Heart and Lung Institute, Imperial College London, Middlesex, UK

[3]School of Life Course Sciences, King's College London, London, UK

[4]CRUK UCL Centre, UCL Cancer Institute, University College London, London, UK

[5]Faculty of Biology, Medicine and Health, University of Manchester, Manchester, UK

Correspondence
Graham M. Lord
Email: graham.lord@manchester.ac.uk

Organ transplantation is often lifesaving, but the long-term deleterious effects of combinatorial immunosuppression regimens and allograft failure cause significant morbidity and mortality. Long-term graft survival in the absence of continuing immunosuppression, defined as operational tolerance, has never been described in the context of multiple major histocompatibility complex (MHC) mismatches. Here, we show that miR-142 deficiency leads to indefinite allograft survival in a fully MHC mismatched murine cardiac transplant model in the absence of exogenous immunosuppression. We demonstrate that the cause of indefinite allograft survival in the absence of miR-142 maps specifically to the T cell compartment. Of therapeutic relevance, temporal deletion of miR-142 in adult mice prior to transplantation of a fully MHC mismatched skin allograft resulted in prolonged allograft survival. Mechanistically, miR-142 directly targets *Tgfbr1* for repression in regulatory T cells (T_{REG}). This leads to increased T_{REG} sensitivity to transforming growth factor – beta and promotes transplant tolerance via an augmented peripheral T_{REG} response in the absence of miR-142. These data identify manipulation of miR-142 as a promising approach for the induction of tolerance in human transplantation.

KEYWORDS

animal models: murine, basic (laboratory) research/science, immunobiology, molecular biology, molecular biology: micro RNA, organ transplantation in general, T cell biology, tolerance: experimental, tolerance: mechanisms

1 | INTRODUCTION

Solid allograft transplantation can be lifesaving at the point of organ failure. However, long-term allograft and patient survival depends on sustained drug-induced immunosuppression. Acute cellular rejection (ACR) occurs in around 25% of heart transplant recipients in the first-year posttransplant despite optimal levels of currently available immunosuppressive therapy, accounting for 10% of mortality in the

first-year posttransplant and increasing the risk of 5-year mortality.[1] Effector $CD4^+$ T cells (T_{EFF}) are critical mediators of allograft responses resulting in allograft rejection. Induction of tolerance is a major goal in transplantation, potentially allowing withdrawal of immunosuppression and indefinite allograft survival.[2] Regulatory T cells (T_{REG}) are a subset of $CD4^+$ T cells that exert dominant suppression of T_{EFF} responses.[3] Peripherally induced T_{REG} cells are critically dependent on transforming growth factor – beta (TGF-β) for the induction of their key transcription factor, FoxP3.[4] The vital role of T_{REGS} in transplant tolerance is apparent where deletion of T_{REGS} in mice already tolerant of kidney allografts leads to allograft rejection.[5] In human studies, the expression of FoxP3 in transplant infiltrating T cells is associated with donor-specific hyporesponsiveness and improved graft histological findings.[6]

MicroRNAs (miRNAs) are short noncoding RNAs that regulate gene expression posttranscriptionally by binding to target sequences on mRNAs, leading to their degradation and/or translational inhibition.[7] The role of miRNAs in the regulation of both innate and adaptive immune responses is increasingly recognized, with aberrant expression of miRNAs contributing to autoimmune diseases and malignancies.[7,8] Recently, we demonstrated a critical role for MicroRNA-142 (miR-142) in regulating peripheral immune tolerance via its action in $CD4^+$ T cells.[9] MiR-142 is highly expressed in cells of hematopoietic lineages, including $CD4^+$ T cells[10] and is conserved across vertebrates, including between humans and mice, supporting the validity of murine models in the investigation of miR-142 function in human disease and therapeutic development.[11] This microRNA exists as two functional isoforms (miR-142-3p and miR-142-5p), capable of binding to different mRNA targets but processed from a single pre-miRNA hairpin. In the context of acute cellular rejection, levels of miR-142-3p and miR-142-5p are consistently increased in cardiac allograft tissue.[12] Serum miR-142-3p levels are also significantly higher in the context of biopsy proven ACR in heart transplant recipients.[13] MiR-142 over-expression is highly predictive of acute T cell–mediated rejection in renal allograft biopsies and is increased in peripheral blood mononuclear cells (PBMC) of patients with chronic antibody-mediated rejection.[14,15] However, miR-142 has also been shown to be up-regulated in B lymphocyte subsets of PBMCs in operationally tolerant renal transplant patients.[16,17] Whether miR-142 actually plays a functional role in transplant rejection and what that role may be, has not previously been explored.

2 | MATERIALS AND METHODS

2.1 | Animals

$Mir142^{fl/fl}$ mice were generated by homologous recombination in 129S mouse embryonic stem cells using a targeted vector containing FRT and loxP sites flanking the $Mir142$ locus and a neomycin resistance cassette (Genoway). Chimeric offspring were bred with C57BL/6J-Flp deleter mice to generate conditional lines, which were fully back-crossed onto a C57BL/6 background. $Cd4^{Cre}$ mice were kindly provided by Professor Matthias Merkenschlager (MRC London Institute of Medical Sciences, Imperial College London). Rosa26-Cre-ER^{T2} transgenic mice were kindly provided by Dr Thomas Ludwig (Columbia University) and generated using the Cre-ER^{T2} construct generated by Pierre Chambon at the Institute of Genetics and Molecular Biology (University of Strasberg). Mice were housed in specific pathogen-free conditions. All experiments were performed according to King's College London and national guidelines, under a UK Home Office Project License (PPL: 70/7869). Appropriate control mice were utilized, with age and sex-matched littermate mice used where possible.

2.2 | Heterotopic heart transplantation

BALB/c (H-2^d) cardiac allografts were transplanted heterotopically into C57BL/6 (H-2^b) recipients that is, a major MHC mismatch (class I and II).[18] Daily palpation of the recipient abdomen for the heterotopic heartbeat, monitoring for signs of slowing or reduced impulse was performed. Allograft rejection was defined as complete cessation of the heterotopic heartbeat. A standard measure of indefinite allograft surgical has been defined as allograft survival of over 100 days.[19,20]

2.3 | In vivo tamoxifen treatment protocol

Rosa26-Cre-ERT2 (ER^{T2}Cre) mice were crossed with $Mir142^{fl/fl}$ animals. Female ER^{T2}Cre$^-$ mice were bred with male ER^{T2}Cre$^{-/+}$ mice. Only ER^{T2}Cre$^{-/+}$ animals were utilized in experiments.

100 μg tamoxifen (Sigma # 156738) diluted in sunflower oil, warmed to 37°C were administered intraperitoneally once daily on 3 consecutive days to ER^{T2}Cre x $Mir142^{fl/fl}$ mice at 5-6 weeks of age.

2.4 | Skin transplantation

Skin transplantation was performed as previously described.[21] Ears of euthanized donor mice were disinfected with 70% ethanol, excised, and split into ventral and dorsal halves. Ventral tissue was kept in phosphate-buffered saline (PBS) on ice prior to implantation and the collagenous ventral flap discarded. Recipient mice were anesthetized by 3% isoflurane inhalation in 100% oxygen at a flow rate of 2 L/min, then maintained using 1.5%-2% isoflurane at 2 L/min intraoperatively. The recipient site was shaved and swabbed with 70% ethanol. A 1-1.5 cm incision was made over the back. The skin graft was then placed atop the graft bed and wrapped in a sterile bandage. The bandage was secured with a single 2-0 silk suture and removed 6-7 days posttransplant.

2.5 | Flow cytometry and intracellular cytokine staining

Spleen and peripheral lymph nodes were processed by tissue disruption and filtration. Following red cell lysis, 5×10^6 splenocytes were stimulated with 50 ng/mL phorbol 12-myristate 13-acetate (PMA) and 1 μg/mL Ionomycin for 4 hours at 37°C, 5% CO_2, with

the addition of 2 μmol/L Monensin for the last 2 hours (Sigma, St. Louis, MO). Anti-mouse CD16/32 antibody was used for Fc-blocking, Live/Dead dyes (Life Technologies, Carlsbad, CA), fluorochrome-conjugated anti-mouse antibodies (eBioscience, San Diego, CA) and anti-Tgfbr1/ anti-Tgfbr2 (R&D Systems, Minneapolis, MN) were used. Intracellular Staining for cytokines was performed after cell fixation and permeabilization using the FoxP3 staining buffer kit (eBioscience). Labelled anti-mouse antibodies to interferon-gamma (IFNγ) and interleukin (IL)-17 (eBioscience) were used. Fluorescence minus one controls were used for gating cytokine expression. Cells were acquired on a BD LSRFortessa (BD Biosciences, San Jose, CA) and data analyzed using FlowJo software (TreeStar, Ashland, OR).

2.6 | Real-time PCR

RNA was extracted using the RNeasy Micro Kit (Qiagen, Hilden, Germany). cDNA was prepared using TaqMan advanced miRNA cDNA synthesis kit (Thermo Fisher Scientific, Waltham, MA). TaqMan fast advanced master mix and TaqMan advanced microRNA Assays were used (Thermo Fisher Scientific) and run on a 7900HT Fast Real-Time PCR system (Thermo Fisher Scientific). U6 small nuclear RNA, miR-191-5p and miR-361 were used as endogenous controls.

2.7 | Alloantibody detection

Serum samples were prepared from 60 μL tail vein bleeds taken at the time of transplant and 14-day intervals. Samples were incubated with anti-CD3-PE (eBioscience) labelled donor (BALB/C) splenocytes (after Fc blockade) with 3-fold serial dilutions of heat-inactivated recipient serum. Cells were then labelled with fluorescein isothiocyanate-labeled goat anti-mouse IgG (Poly4053) (BioLegend, San Diego, CA) and acquired on a FACS Canto machine (BD Biosciences). Sera from wild-type recipients of fully allogeneic allografts and naïve animals were used as positive and negative controls respectively.

2.8 | Histology

Samples were fixed in 10% neutral buffered formalin for 48 hours before paraffin-embedding and sectioning. Histological scoring was performed blinded according to the International Society for Heart and Lung Transplantation standardizing grading criteria for the diagnosis of heart rejection[22] and the Banff 2007 working classification of skin allograft pathology.[23] Microscopy was performed with an Olympus BX51 microscope.

2.8.1 | Hematoxylin & eosin staining

5 mm thick sections were dewaxed, rehydrated with water, then stained with Mayer's hematoxylin for 5 minutes, washed and incubated with 1% Eosin stain for 5 minutes, rinsed briefly with tap water, dehydrated rapidly through graded methanol, cleared in Xylene and mounted in DPX.

2.8.2 | Masson trichrome staining

5 mm thick sections were stained with Celestine Blue for 5 minutes, washed, incubated in hemotoxylin for 5 minutes and washed in tap water for 5 minutes. Slides were then incubated with Acid Fucsin for 5 minutes, rinsed quickly in distilled water, differentiated in Phosphomolybdic acid (1%) for 3-5 minutes, then rinsed briefly in water prior to staining in Methyl Blue for 2-3 minutes. Slides were washed briefly with distilled water and dehydrated in ascending series of methanol, cleared in xylene and mounted in DPX (VWR).

2.9 | Immunohistochemistry

2.9.1 | Immunoperoxidase staining

5 μm thick paraffin wax samples were dewaxed and rehydrated with water. Endogenous peroxidases were blocked with 3% hydrogen peroxide for 5 minutes. Antigen retrieval was carried out in 0.1 mol/L citrate buffer (pH 6) with microwaving for 10 minutes. Samples were washed in water and incubated with 3% Bovine serum albumin (BSA; Sigma) for 30 minutes, then incubated overnight in a moist chamber with antibody against C4d (rabbit polyclonal, Hycult biotech, HP8033) or Foxp3 (rabbit polyclonal, Novus Biologicals, Littleton, CO, NB100-39002). Negative controls consisted of 3% BSA in PBS. After washing, samples were incubated with biotinylated goat anti-rabbit IgG for 60 minutes followed by Avadin-Biotin-peroxidase Complex (ABC) (Vector Laboratories, Burlingame, CA) for 30 minutes. Specimens were incubated with DAB (Sigma) for 5 minutes, washed with water and stained with Hematoxylin for 1 minute and mounted using Aquatex (VWR). Slides were viewed on a Ziess Axioskop microscope and digital micrographs taken using a Nikon DMX1200 camera. Five random areas of the skin were imaged at ×40 magnification and manually counted using image J software (nonblinded).[24]

2.9.2 | Immunofluorescence colocalization staining

5 mm thick paraffin wax sections of skin tissue were dewaxed and rehydrated with water. Antigen retrieval was carried out by immersing the slides in Tris-EDTA buffer buffer (pH 9) and microwaving for 10 minutes. Samples were left in the same buffer for 20 minutes followed by tap water wash. Slides were incubated with 3% Bovine serum albumin (BSA -Sigma) for 30 minutes and incubated overnight in a moist chamber with antibodies against CD4 (rabbit monoclonal, 1:300 dilution, Abcam) and FoxP3 (rat monoclonal, 1:50 dilution, Invitrogen). Negative controls consisted of matched rat and rabbit
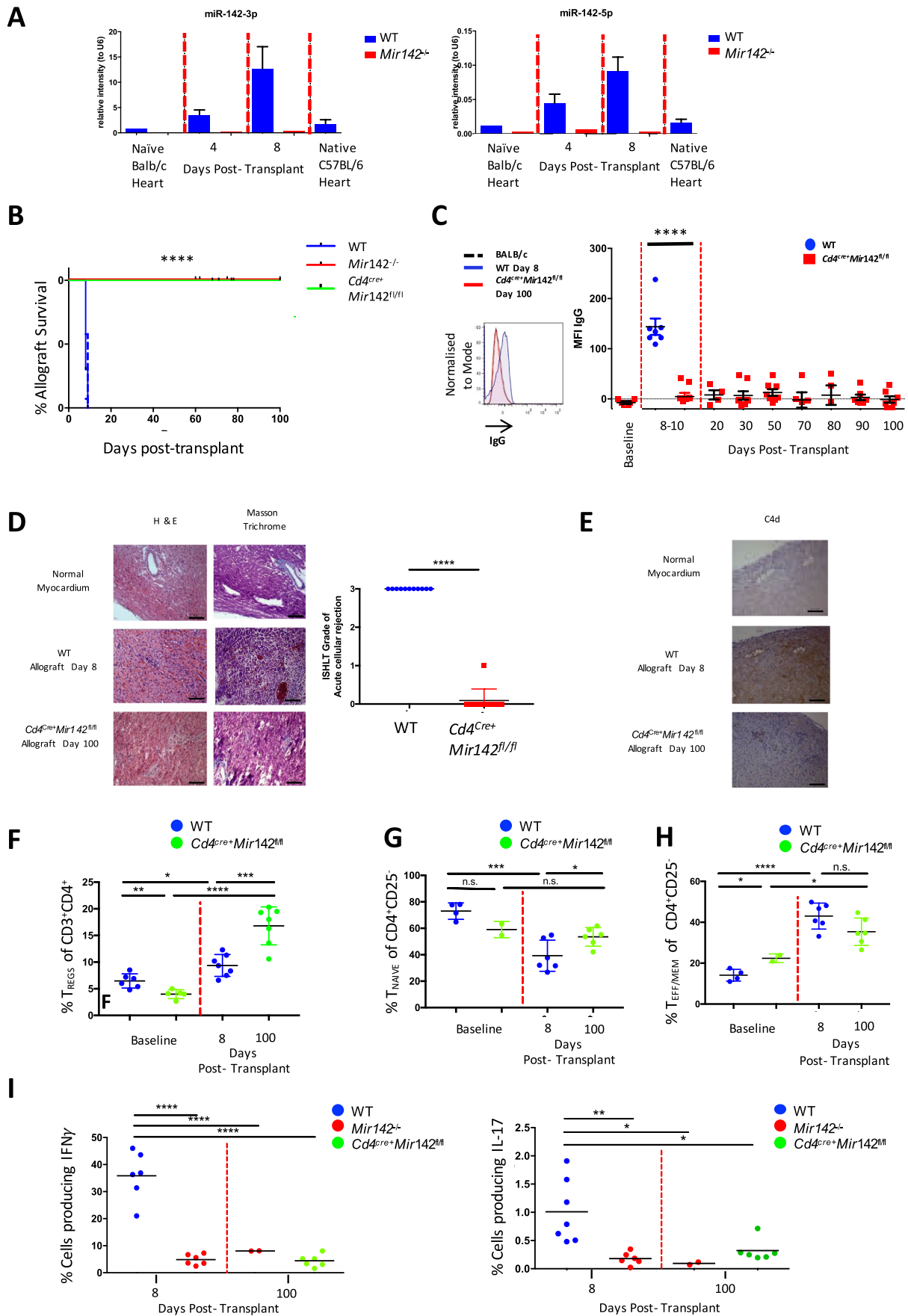
FIGURE 1 miR-142 plays a critical role in allograft survival, which maps specifically to the T cell compartment. A, miR-142-3p and miR-142-5p levels in allograft samples, measured by real-time polymerase chain reaction (RT-qPCR). B, Kaplan Meier allograft survival chart of $Mir142^{-/-}$ (n = 6), $Cd4^{cre+}Mir142^{fl/fl}$ (n = 11) vs wild type (WT) (n = 11) mice (Mantel-Cox test ****P < .0001). C, Donor-specific antibody responses over time in $Cd4^{cre+}Mir142^{fl/fl}$ vs WT mice (n > 5 per group; Student's t test ****P < .0001). D, Hematoxylin and eosin (H&E) and Masson Trichrome staining of formalin fixed, paraffin embedded (FFPE) sections from allografts from $Cd4^{cre+}Mir142^{fl/fl}$ and WT recipients (magnification ×10; scale bar 100 µm) (left); International Society for Heart and Lung Transplantation grade of acute cellular rejection of heart allograft[22] (right) (n = 11; Student t test; ****P < .0001). E, C4d staining of FFPE sections from allografts from $Cd4^{cre+}Mir142^{fl/fl}$ and WT recipients (magnification ×10; scale bar 100 µm). F, Percentage of $CD4^+ CD25^+$ T_{REGS} (n > 5; one way ANOVA; *P < .05, **P < .01, ***P < .001, ****P < .0001). G, Percentage of T_{NAIVE} ($CD4^+CD25^-CD62L^{high} CD44^{low}$) cells (n > 2 pretransplant and n = 6 posttransplant; one way ANOVA; *P < .05, **P < .01, ***P < .001). H, Percentage of $T_{EFF/MEM}$ ($CD4^+CD25^-CD44^{high}CD62L^{low}$) cells (n > 2 pretransplant and n = 6 posttransplant; one way ANOVA; *P < .05, **P < .01, ****P < .0001). I, Direct ex vivo interferon-gamma (IFNɣ) and interleukin (IL)-17 cytokine responses in $CD3^+CD4^+$ T cells at day 8 and day 100 posttransplant (n > 2; one way ANOVA; *P < .05, **P < .01, ****P < .0001)

antibody isotypes. After washing, specimens were incubated with goat anti-rabbit AlexaFluor 488 and goat anti-rat AlexaFluor 594 respectively (Life Technologies) for 1 hour. After washing three times with PBS, sections were incubated with DAPI (sigma) and mounted using Permafluor (Thermo Fisher). Stained sections were imaged using a Zeiss LSM 880 confocal microscope.

2.10 | Western blot

FACS purified naïve $CD4^+$ T cells were activated with plate-bound anti-CD3 (2 µg/mL) and anti-CD28 (3 µg/mL) antibodies (Bio X Cell), and cultured for 30, 60 and 120 minutes in serum-free medium at 37°C in the presence of recombinant human IL-2 (20 ng/mL) (R&D Systems) and TGF-β1 (3 ng/mL) (Promokine). Cells were prepared as previously described[9] and probed with rabbit anti-mouse Smad2/3, Smad4, Smad 7, phospho-Smad2/3 and beta-actin (Cell Signeling). HRP-conjugated goat anti-rabbit IgG was used for secondary detection (GE Healthcare, Chicago, IL). Blots were developed using enhanced chemiluminenscence (Thermo Scientific/Pearce). Intensity was quantified using Genetools software (Syngne) and expressed as fold increase above basal level.

2.11 | Statistical analysis

Statistical analysis was carried out using GraphPad Prism 7 (GraphPad Software). P < .05 was considered statistically significant and represented in figures as (*), with P < .01 represented in figures as (**), P < .001 represented as (***) and P < .0001 represented as (****).

3 | RESULTS

3.1 | miR-142 plays a critical role in the tolerogenic response to an allograft, specifically via the T cell compartment

MiR-142 levels are raised in the context of acute rejection of renal and cardiac transplants in humans.[12] Therefore, we assessed miR-142

levels in allograft tissue in a murine heart transplant model of acute humoral and cellular rejection known to result in robust acute humoral and cellular rejection, with high circulating IgG alloantibody levels, and graft failure within 10 days.[18]

At day 4 posttransplant, miR-142-3p and miR-142-5p were increased in the allografts of wild type (WT) recipients, with a further increase at day 8 posttransplant (Figure 1A). To understand how rejection might take place in an environment deficient for this miRNA, we generated and validated constitutive miR-142 deficient mice via Cre-mediated recombination ($Mir142^{-/-}$) (Figure S1A-D). When these animals were subjected to heterotopic heart transplantation, recipients demonstrated indefinite allograft survival (>100 days) in the absence of exogenous immunosuppression, with WT recipients rejecting at the expected time of under 10 days (Figure 1B). Intriguingly, we observed the same phenomenon when mice with a T cell-conditional deletion of miR-142 ($Cd4^{cre+}Mir142^{fl/fl}$: Figure S1A-D) were subjected to the same model, demonstrating that the effects of miR-142 mapped specifically to the T cell compartment. Monitoring of donor-specific antibody response revealed absent donor-specific IgG alloantibody in both $Cd4^{cre+}Mir142^{fl/fl}$ and the $Mir142^{-/-}$ recipients. In contrast, WT recipients exhibited significantly increased alloantibody responses at the time of rejection (Figure 1C; Figure S2B). Furthermore, histological evidence of perivascular infiltrate, myocyte damage and hemorrhage seen in WT allografts were entirely absent in both $Cd4^{cre+}Mir142^{fl/fl}$ and $Mir142^{-/-}$ recipients (Figure 1D; Figure S2A). Immunohistochemical staining for C4d also revealed no deposition in myocytes and the endothelium of $Cd4^{cre+}Mir142^{fl/fl}$ recipient allografts, supporting an absence of a humoral response to the allograft in the absence of T cell intrinsic miR-142 expression (Figure 1E). Additionally, to determine if this phenomenon was due to donor or recipient effects, allografts from $Mir142^{-/-}$ donors were transplanted into BALB/c recipients. Importantly, $Mir142^{-/-}$ donors were rejected at the same rate as WT donors (Figure S3).

Further characterization of the $CD4^+$ T cell compartment using $Cd4^{cre+}Mir142^{fl/fl}$ and WT mice demonstrated that in both genotypes, $CD4^+$ T cell populations responded appropriately to an allograft, with an increased peripheral T_{REG} pool (Figure 1F) and a reduction in the $CD4^+CD25^-CD44^{low}CD62L^{high}$ naïve T cell (T_{NAIVE}) population (Figure 1G), concomitant with an increase in T cells displaying an effector/memory phenotype ($T_{EFF/MEM}$) (Figure 1H). However, at

A

B

C

D

CD4 – Green   Fox P3 – Red   Nucleus – Blue   Merged – Purple

E

F
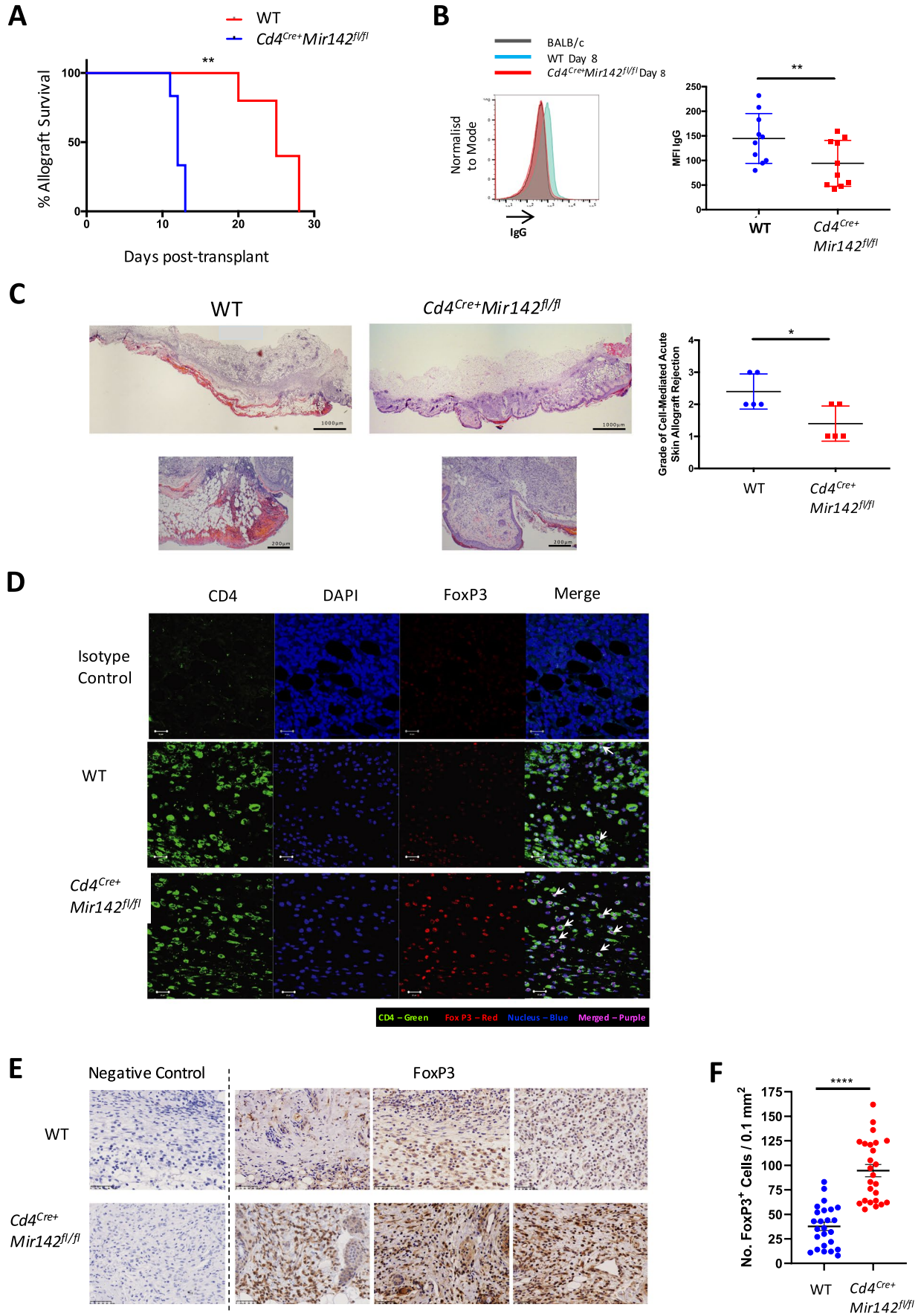
FIGURE 2 Prolonged skin allograft survival in *Cd4Cre+Mir142fl/fl* mice. A, Kaplan Meier allograft survival chart of wild type (WT) vs *Cd4Cre+Mir142fl/fl* mice (n > 8 per group, Mantel-Cox test **P < .01). B, Donor-specific antibody responses WT vs *Cd4Cre+Mir142fl/fl* at day 8 posttransplant (n > 8 per group; **P < .01; unpaired two-tailed *t* test). C, Hematoxylin and eosin (H&E) staining of formalin fixed, paraffin embedded (FFPE) sections from allografts from WT and *Cd4Cre+Mir142fl/fl* recipients at day 8 posttransplant (scale bars 1000 and 200 μm) (left); Banff grading of cell-mediated skin allograft rejection[23] (n = 5; Student's *t* test; *P < .05) (right). D, Representative immunofluorescence images of CD4 (green), FoxP3 (red), DAPI (blue), Merged cells (purple) of allografts from WT and *Cd4cre+Mir142fl/fl* recipients at day 8 posttransplant with isotype controls (scale bar 20 μm; arrows indicate merged cells). E, Representative immunoperoxidase images of FoxP3 positive cells of allografts from n = 3 WT and n = 3 *Cd4cre+Mir142fl/fl* recipients at day 8 posttransplant (scale bar 50 μm)

day 100 posttransplant, *Cd4cre+Mir142fl/fl* mice showed a significant increase in the T_{REG} population (Figure 1F) with a higher proportion of CD4$^+$ T cells retaining a T_{NAIVE} phenotype (Figure 1G) compared with WT mice at the time of rejection (day 8). Critically, direct ex vivo intracytoplasmic cytokine capture (ICC) of splenocytes from WT allograft recipients at the time of allograft rejection revealed robust expression of IFN-γ, in addition to IL-17 production by CD4$^+$ T cells, while there was no increase in CD4$^+$ T cell IFN-γ and IL-17 production in *Cd4cre+Mir142fl/fl* recipients at day 8 or day 100 posttransplant; this was also true of *Mir142−/−* animals (Figure 1I).

3.2 | T cell intrinsic miR-142 deficiency prolongs skin allograft survival

Given the striking results observed in our heterotopic heart transplantation model, we opted to examine the outcome of T cell miR-142 deficiency in a fully MHC mismatched (Class I and II) skin transplant model; difficulties in prolonging allograft survival is a well-documented characteristic of this model.[25,26] Despite this, *Cd4cre+Mir142fl/fl* recipients demonstrated prolonged allograft survival (MST 25 days vs 12 days, P < .01) without any exogenous treatment (Figure 2A). Significantly reduced donor-specific antibody responses in *Cd4cre+Mir142fl/fl* recipients compared with control mice at day 8 posttransplant, indicated an attenuated humoral response (Figure 2B). Comparison of histological findings at day 8 posttransplant revealed markedly reduced lymphohistocytic infiltration and hemorrhage in *Cd4cre+Mir142fl/fl* animals[24] (Figure 2C). Importantly, immunohistochemical (IHC) analysis revealed CD4$^+$ T cell infiltrate in the allografts of both groups (Figure 2D). However, co-staining for FoxP3 appeared qualitatively far more robust and profuse in allografts of *Cd4cre+Mir142fl/fl* recipients. This was supported by IHC-P analysis showing more extensive and robust FoxP3 expression in skin allografts *Cd4cre+Mir142fl/fl* (Figure 2E), with quantification confirming increased T_{REG} infiltration in *Cd4cre+Mir142fl/fl* recipients compared to WT controls (Figure 2F). In addition, more extensive FoxP3 expression was observed in *Cd4cre+Mir142fl/fl* recipient cardiac allografts taken from the model outlined in Figure 1F (Figure S4). These data suggest that in response to exposure to an allograft, an enhanced T_{REG} response is generated by the absence of miR-142 isoforms.

Deletion of miR-142 either constitutively or conditionally via *Cd4*-driven deletion in thymocyte T cell precursors, poses the possibility that typical T cell development may be compromised in the absence of this microRNA. To overcome this, we generated a ER^{T2}Cre

transgenic[27,28] deletion model (ER^{T2}Cre+*Mir142fl/fl*), in which deletion of *Mir142* could be temporally controlled through the administration of tamoxifen in vivo (Figure S5A,B). Temporal deletion of *Mir142* did not grossly alter the peripheral lymphocyte pool, as determined by B:T cell and CD4:CD8 T cell ratios (Figure S6A,B), or negatively impact T cell viability (Figure S6C).

Analogous to our findings in *Cd4cre+Mir142fl/fl* mice, ER^{T2}Cre+*Mir142fl/fl* recipients demonstrated prolonged allograft survival compared to *Mir142fl/fl* littermate controls (MST 15 days vs 9.5 days, P < .0001) (Figure 3A,B). Comparison of histological findings at day 8 posttransplant revealed reduced lymphohistocytic infiltration and hemorrhage in ER^{T2}Cre+*Mir142fl/fl* animals (Figure 3C). As before, we found a significant increase in the proportion of CD4$^+$CD25$^+$ T_{REGS} (Figure 3D) and decrease in $T_{EFF/MEM}$ populations in ER^{T2}Cre+*Mir142fl/fl* mice when compared with control mice at day 8 in secondary lymphoid tissue sites (Figure 3D,E). Directly ex vivo ICC revealed significantly reduced CD4$^+$ T cell production of IFN-γ and IL-17 production at day 8 (Figure 3F). Similarly, donor-specific antibody responses were significantly reduced in ER^{T2}Cre+*Mir142fl/fl* mice when compared with control mice (Figure 3G).

3.3 | Expression of the miR-142-3p target *Tgfbr1* is increased in miR-142 deficient T_{REG} and augments sensitivity to TGF-β signaling

In all the transplantation models we had explored, an enhanced T_{REGS} response was apparent in the context of T cell miR-142 deficiency. Therefore, we reasoned that the absence of miR-142 in the context of exposure to an allograft may promote a more tolerogenic environment, via mechanisms which augment T_{REG} development and subsequent dominant tolerance.

Among factors which promote T_{REG} development and function, the TGF-β signaling pathway plays an important role, not least by promoting the expression of *Foxp3*.[29,30] TGF-β signals via a heterodimeric receptor composed of ALK5 (Tgfbr1) and the subunit Tgfbr2. Interestingly, the 3'UTR of *Tgfbr1* mRNA contains a highly conserved seed sequence for miR-142-3p and the 3'UTR of *Tgfbr2* mRNA contains a highly conserved seed sequence for miR-142-5p (Figure S7A,B). miR-142 regulation of the expression of *Tgfbr1* and *Tgfbr2* has been validated in several cell types including hematopoietically derived lineages.[31-36]

To determine whether miR-142 deficient T cells exhibited increased levels of Tgfbr1 and Tgfbr2, we utilized the T cell-conditional miR-142 deficient model of skin allograft transplantation. At
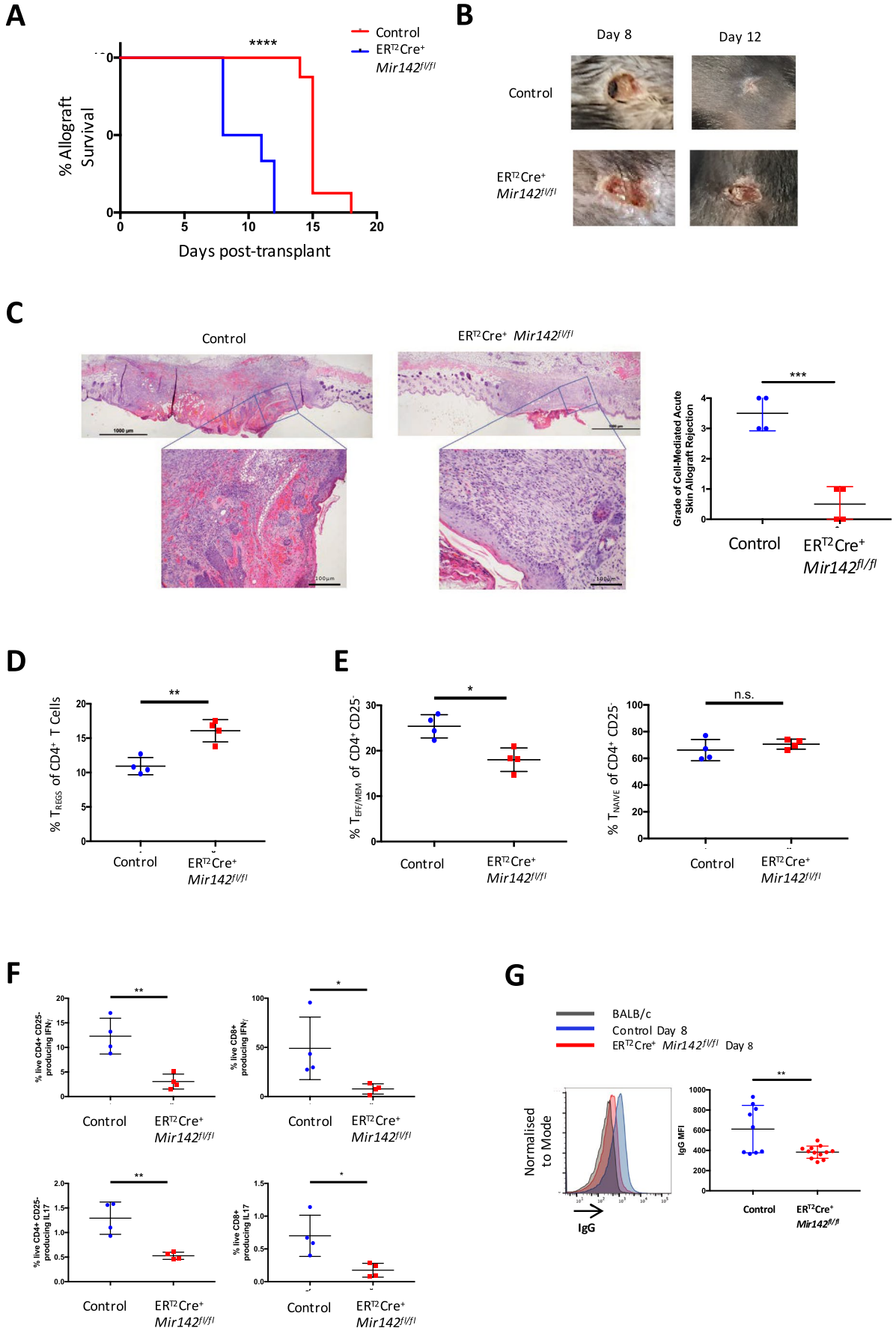
FIGURE 3 Prolonged skin allograft survival in ER^{T2}Cre$^+$Mir142$^{fl/fl}$ mice. A, Kaplan Meier allograft survival chart of control vs ER^{T2}Cre$^+$Mir142$^{fl/fl}$ littermates (n > 8 per group, Mantel-Cox test ****P < .0001). B, Macroscopic appearance of control vs ER^{T2}Cre$^+$Mir142$^{fl/fl}$ skin allografts at days 8 and 12. C, Hematoxylin and eosin (H&E) staining of formalin fixed, paraffin embedded (FFPE) sections from allografts from ER^{T2}Cre$^+$Mir142$^{fl/fl}$ and control recipients at day 8 posttransplant (magnification ×5 and ×20; scale bars 1000 and 100 μm) (left); Banff grading of cell-mediated skin allograft rejection[23] (n = 5; Student's t test; ***P < .001) (right). D, Percentage of T$_{REG}$ (CD4$^+$ CD25$^+$) (n = 4; Mann-Whitney U test, **P < .01). E, Percentage of T$_{EFF/MEM}$ (CD4$^+$CD25$^-$CD44^{high}CD62L^{low}) cells (left) and percentage of T$_{NAIVE}$ (CD4$^+$CD25$^-$CD62L^{high}CD44^{low}) (right) (n = 4; Mann-Whitney U test, *P < .05). F, Direct ex vivo interferon-gamma (IFNγ) and interleukin (IL)-17 cytokine responses in CD3$^+$CD4$^+$ and CD3$^+$CD8$^+$ T cells at day 8 posttransplant (n = 4 per group; *P < .05, **P < .01; unpaired two-tailed t test). G, Donor-specific antibody responses, control vs ER^{T2}Cre$^+$Mir142$^{fl/fl}$ at day 8 posttransplant (n > 8 per group; **P < .01; unpaired two-tailed t test)

8 days posttransplant, Cd4^{cre+}Mir142$^{fl/fl}$ animals and WT controls were sacrificed, and peripheral lymph nodes and spleen populations of T cells were analyzed for Tgfbr1 and Tgfbr2 expression by flow cytometry. In both sites, Tgfbr1 surface expression was significantly enhanced on T$_{REGS}$, whereas Tgfbr2 expression was unaffected (Figure 4A,B). In contrast, CD4$^+$ T cells (T$_{CONV}$) did not demonstrate enhanced Tgfbr1 expression in the lymph nodes, although a small increase was observed in the spleen. Interestingly, at both sites, a significant downregulation of Tgfbr2 expression was noted for T$_{CONV}$ (Figure 4A,B). Furthermore, despite similar levels of total Smad2/3 protein between the genotypes (Figure 4C,D) and comparable levels of inhibitory Smad7 (Figure 4C,F), CD4$^+$ T cells isolated from secondary lymphoid sites of Cd4^{cre+}Mir142$^{fl/fl}$ animals demonstrated enhanced pSmad2 (Ser465/467)/Smad3(Ser423/425) when activated in the presence of TGF-β1 compared to WT controls (Figure 4C,F).

4 | DISCUSSION

We have demonstrated that the absence of miR-142 induces indefinite cardiac allograft survival across full MHC (Class I and II) mismatches, caused by a T cell-specific mechanism, which promotes dominant tolerance and suppression of effector CD4$^+$ T cell responses via the enhancement of the peripheral T$_{REG}$ response.

Diminished T cell numbers in secondary lymphoid organs have been observed in Mir142$^{-/-}$ mice.[37,38] We also found this to be the case in our constitutive and T cell-conditional knockout lines at baseline (data not shown). However, CD4 and CD8 deficient mice as well as Rag$^{-/-}$ mice, which lack T and B cells, can vigorously reject skin allografts at the same rate as WT mice.[39-42] B6 μMT$^{-/-}$ mice are B cell-deficient with a paucity of CD4$^+$ T cells yet are still capable of rejecting skin and heart allografts.[41,43] Importantly, as few as 1 × 10^3 donor-specific T cells are capable of rejecting skin allografts.[25,44] The quantitatively similar responses to the allograft in our mice, which are only partially T cell-deficient and possess T cells in their peripheral tissues, indicates that this is unlikely to contribute significantly to the observed long-term transplant survival.

The strength of T$_{EFF/MEM}$ responses in both lymphoid and non-lymphoid tissues is a barrier to transplant tolerance.[45,46] The presence and number of alloantigen-specific T$_{EFF/MEM}$ cells in humans correlates with worse transplant outcomes.[47] Despite current immunosuppressive regimens capable of non-specific T cell depletion,

certain T$_{EFF/MEM}$ subsets have been found to survive treatment with the commonly used depleting induction agents, Campath (anti-CD52 mAb) or anti-thymocyte globulin. Indeed, these cells expand and proliferate in the "empty" host to play a prominent role in acute rejection.[48] Other attempts to augment allograft survival using co-stimulatory blockade (eg, CD28/B7) have had limited success due to the presence of alloreactive memory T cells. In fact, few strategies have resulted in the induction of transplant tolerance. Chronic allograft rejection is also associated with decreased CD4$^+$CD25$^+$ T$_{REGS}$ and reduced Foxp3 transcripts in PBMCs compared with both healthy controls and operationally tolerant recipients, indicating the importance of maintenance of the T$_{REG}$ population for allograft survival.[49] In murine studies, increasing the number of T$_{REGS}$ can adoptively transfer transplant tolerance and expansion of the T$_{REG}$ population has been shown to occur in the periphery to mediate this phenomenon.[50-52] To address the question of the functional capacity of these T$_{REGS}$, three separate studies used autologous, polyclonal or donor-specific T cell stimulation in T$_{REG}$ suppression assays. The authors concluded that these T$_{REGS}$ are fully functional and propose that it is the proportion rather than any altered suppressive ability of T$_{REGS}$ that determines allograft outcome.[49,53,54] A number of human and murine studies demonstrated that miR-142 expression is increased in the context of acute allograft rejection[12,13,55] and in light of the above studies, the shift in the balance of T$_{REG}$ and T$_{EFF/MEM}$ populations in response to an allograft in the absence of miR-142 is likely to be of crucial importance.

There have been conflicting reports on the level of TGF-β1 mRNA in operationally tolerant patients. However, the TGF-β signaling pathway has been shown to regulate the function of 27% of the genes that are associated with operationally tolerant patients in blood samples.[56,57] Previously, TGF-β signaling in T cells has been shown to promote long-term skin allograft acceptance in a model of minor MHC mismatch[58] and, in conjunction with co-receptor blockade, TGF-β has also been shown to promote induction of Foxp3 and maintenance of transplant tolerance in monospecific TCR-transgenic mice.[59] Enhanced expression of FOXP3, TGFB1 and TGFBR1 in PBMC of operationally tolerant renal transplant patients compared with renal transplant recipients not exhibiting operational tolerance, indicate the significance of this signaling pathway in transplant tolerance.[17,57] Several studies have shown that miR-142 plays a critical and highly conserved role in regulating TGF-β receptor signaling in vertebrates.[31-36] Upregulation of Tgfbr1 expression in CD4$^+$CD25$^+$FoxP3$^+$ T$_{REGS}$ from mice with T$_{REG}$-conditional deletion
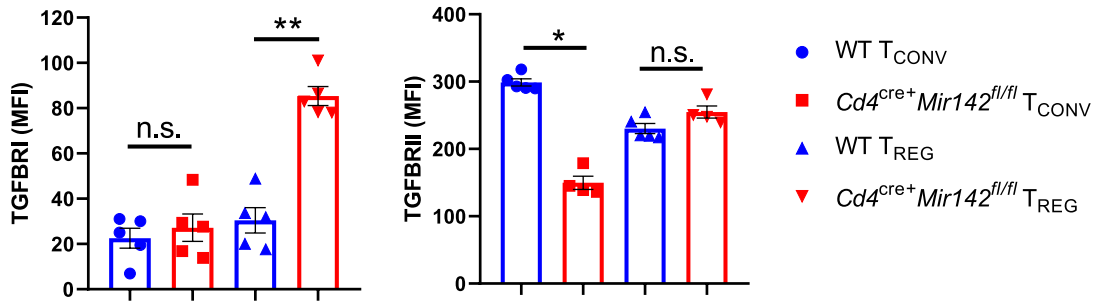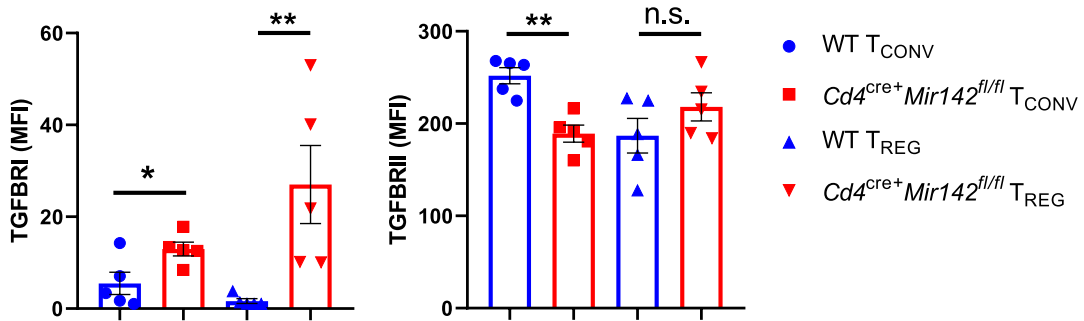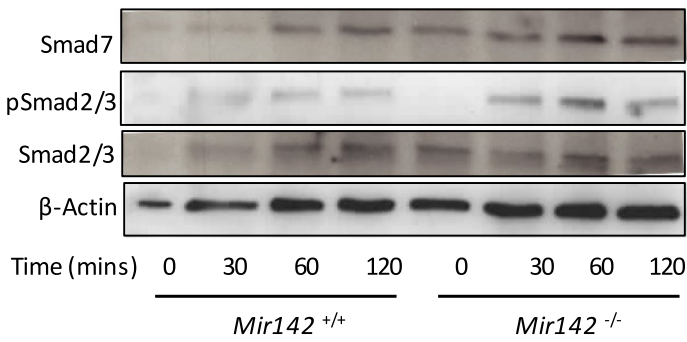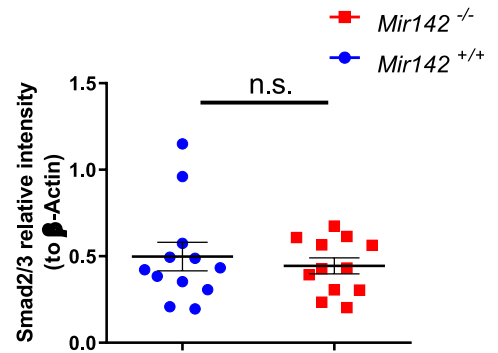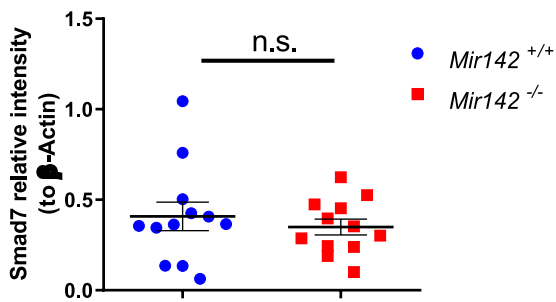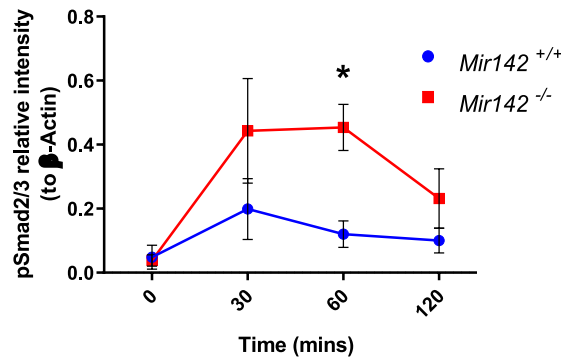
FIGURE 4 Expression of miR-142-3p target *Tgfbr1* is increased in miR-142 deficient CD4$^+$CD25$^+$ T$_{REG}$ following skin allograft transplantation and increases cell sensitivity to transforming growth factor (TGF)-β1 signaling. A, Mean fluorescence intensity (MFI) of anti-Tgfbr1 and anti-Tgfbr2 staining on CD4$^+$CD25$^-$ T$_{CONV}$ and CD4$^+$CD25$^+$ T$_{REG}$ from peripheral lymph nodes, 8 d posttransplant with BALB/C skin allografts of wild type (WT; C57B6/J) and *Cd4*$^{cre+}$*Mir142*$^{fl/fl}$ mice. B, MFI of anti-Tgfbr1 and anti-Tgfbr2 staining on CD4$^+$CD25$^-$ T$_{CONV}$ and CD4$^+$CD25$^+$ T$_{REG}$ from spleen of WT (C57B6/J) and *Cd4*$^{cre+}$*Mir142*$^{fl/fl}$ mice, 8 d posttransplant with BALB/C skin allografts. C, Representative western blot images demonstrating Smad7, phospho-Smad2 (Ser465/467)/Smad3(Ser423/425), Smad2/3, and β-Actin protein expression over time (0-120 min) in CD4$^+$ T cells isolated from spleen and peripheral lymph nodes of *Mir142*$^{+/+}$ and *Mir142*$^{-/-}$ mice treated with exogenous TGF-β1, interleukin (IL)-2 and activated with anti-CD3/anti-CD28 monoclonal antibodies in vitro. D, Cumulative western blot data from 3 independent experiments for Smad2/3 and (E) Smad7 relative intensity to β-Actin expression, combining data from all time points. F, Cumulative western blot data from 3 independent experiments for pSmad2/3 relative to β-Actin over time. All data are represented as mean ± SEM Each data point in (A,B) represents 1 mouse (n = 5). MFI values calculated by subtracting Tgfbr1 and Tgfbr2 fluorescence minus one control MFI values from corresponding sample values. Mann-Whitney *U* test (A,B)/Student's *t* test (D-F), *P < .05, **P < .01, n.s. >0.05, nonsignificant

of *Mir142*, in combination with the highly conserved seed sequences for miR-142-3p in the 3′UTR of *Tgfbr1* make this a plausible target for miR-142-3p in T$_{REG}$.[11]

In contrast to our previous findings, where we found that the absence of miR-142 specifically in FoxP3$^+$ T$_{REGS}$ results in a lethal, multi-system autoimmune disease and impaired T$_{REG}$ suppressive function,[9] here we found that the absence of miR-142 in T cells results in indefinite allograft survival and the augmented generation and/or survival of T$_{REGS}$. This surprising finding may be explained by putative de novo generation of a large number of alloantigen-specific T$_{REG}$ in the context of a transplant, driven by enhanced TGF-β signaling mediated by the absence of miR-142-3p. Previously we showed aberrant immune responses to nominal self-antigens is mediated by miR-142-5p regulation of *Pde3b*. Whether this difference reflects the differential expression of the -3p and -5p strand of miR-142 in separate T$_{REG}$ subsets (eg, thymic T$_{REG}$ vs peripheral T$_{REG}$) in response to self vs nonself-antigens remains to be determined.

In summary, miRNAs have emerged as key regulators of numerous biological processes. Our data identify that miR-142 plays a critical role in solid organ transplantation, modulating expression of its target *Tgfbr1* in T$_{REGS}$, thereby modulating T$_{REG}$ sensitivity to TGF-β and promoting transplant tolerance via augmented T$_{REG}$ development. These findings suggest that targeted T$_{REG}$ therapy aimed at manipulation of miR-142 and its target *TGFBR1* could have therapeutic potential in improving allograft survival.

DATA AVAILABILITY STATEMENT

The data that support the findings of this study are available from the corresponding author upon reasonable request.

ORCID

Nelomi Anandagoda https://orcid.org/0000-0003-2975-4351
Luke B. Roberts https://orcid.org/0000-0003-1143-304X
Joanna C. D. Willis https://orcid.org/0000-0003-3260-4311
Padmini Sarathchandra https://orcid.org/0000-0001-9331-3046
Fang Xiao https://orcid.org/0000-0002-8978-2461
Ian Jackson https://orcid.org/0000-0003-3600-7784
Arnulf Hertweck https://orcid.org/0000-0002-8609-8146
Puja Kapoor https://orcid.org/0000-0001-6027-1038
Richard G. Jenner https://orcid.org/0000-0002-2946-6811
Jane K. Howard https://orcid.org/0000-0003-2754-8300
Graham M. Lord https://orcid.org/0000-0003-2069-4743

REFERENCES

1. Soderlund C, Öhman J, Nilsson J, et al. Acute cellular rejection the first year after heart transplantation and its impact on survival: a single-centre retrospective study at Skåne University Hospital in Lund 1988–2010. *Transpl Int*. 2014;27:482-492.
2. Martínez-Llordella M, Lozano JJ, Puig-Pey I, et al. Using transcriptional profiling to develop a diagnostic test of operational tolerance in liver transplant recipients. *J Clin Invest*. 2008;118:2845-2857.
3. Kronenberg M, Rudensky A. Regulation of immunity by self-reactive T cells. *Nature*. 2005;435:598-604.
4. Chen W,Jin W, Hardegen N, et al. Conversion of peripheral CD4+CD25- naive T cells to CD4+CD25+ regulatory T cells by TGF-beta induction of transcription factor Foxp3. *J Exp Med*. 2003;198(12):1875-1886.

5. Miyajima M, Chase CM, Alessandrini A, et al. Early acceptance of renal allografts in mice is dependent on foxp3(+) cells. *Am J Pathol.* 2011;178(4):1635-1645.

6. Bestard O, Cruzado JM, Mestre M, et al. Achieving donor-specific hyporesponsiveness is associated with FOXP3+ regulatory T cell recruitment in human renal allograft infiltrates. *J Immunol.* 2007;179:4901-4909.

7. Guo H, Ingolia NT, Weissman JS, Bartel DP. Mammalian microR-NAs predominantly act to decrease target mRNA levels. *Nature.* 2010;466:835-840.

8. O'Connell RM, Rao DS, Chaudhuri AA, et al. Physiological and pathological roles for microRNAs in the immune system. *Nat Rev Immunol.* 2010;10:111-122.

9. Anandagoda N, Willis JCD, Hertweck A, et al. MicroRNA-142–mediated repression of phosphodiesterase 3B critically regulates peripheral immune tolerance. *J Clin Invest.* 2019;129(3):1257-1271.

10. Landgraf P, Rusu M, Sheridan R, et al. A mammalian microRNA expression atlas based on small RNA library sequencing. *Cell.* 2007;129(7):1401-1414.

11. miRBase release 22.1 microRNA annotation and deep-sequencing data web site. http://www.mirbase.org. Updated October 2018. Accessed August 2019.

12. Van Aelst LNL, Summer G, Li S, et al. RNA profiling in human and murine transplanted hearts: identification and validation of therapeutic targets for acute cardiac and renal allograft rejection. *Am J Transplant.* 2016;16(1):99-110.

13. Sukma Dewi I, Hollander Z, Lam KK, et al. Association of serum MiR-142-3p and MiR-101-3p levels with acute cellular rejection after heart transplantation. *PLoS ONE.* 2017;12(1):e0170842.

14. Anglicheau D, Sharma VK, Ding R, et al. MicroRNA expression profiles predictive of human renal allograft status. *Proc Natl Acad Sci USA.* 2009;106(13):5330-5335.

15. Danger R, Paul C, Giral M, et al. Expression of miR-142-5p in peripheral blood mononuclear cells from renal transplant patients with chronic antibody-mediated rejection. *PLoS ONE.* 2013;8(4):e60702.

16. Ben-Dov IZ, Muthukumar T, Morozov P, et al. MicroRNA sequence profiles of human kidney allografts with or without tubulointerstitial fibrosis. *Transplantation.* 2012;94(11):1086-1094.

17. Danger R, Pallier A, Giral M, et al. Upregulation of miR-142-3p in peripheral blood mononuclear cells of operationally tolerant patients with a renal transplant. *J Am Soc Nephrol.* 2012;23(4):597-606.

18. Yin H, Li X-Y, Jin X-B, et al. IL-33 prolongs murine cardiac allograft survival through induction of TH2-type immune deviation. *Transplantation.* 2010;89(10):1189-1197.

19. Cranston D, Wood KJ, Morris PJ. Splenectomy and renal allograft survival in the rat. *Br J Surgery.* 1988;75(1):18-22.

20. Tchervenkov JI, Cofer BR, Davies C, Alexander JW. Indefinite allograft survival induced by the combination of multiple donor-specific transfusions, cyclosporine, and an anti-T cell monoclonal antibody in a protocol relevant to cadaveric organ transplantation. The importance of prolonged posttransplant cyclosporine coverage. *Transplantation.* 1995;59(6):821-824.

21. Garrod KR, Cahalan MD. Murine skin transplantation. *J Vis Exp.* 2008;(11): pii: 634. https://doi.org/10.3791/634

22. Stewart S, Winters GL, Fishbein MC, et al. Revision of the 1990 working formulation for the standardization of nomenclature in the diagnosis of heart rejection. *J Heart Lung Transplant.* 2005;24(11):1710-1720.

23. Cendales LC, Kanitakis J, Schneeberger S, et al. The Banff 2007 working classification of skin-containing composite tissue allograft pathology. *Am J Transplant.* 2008;8(7):1396-1400.

24. Schindelin J, Arganda-Carreras I, Frise E, et al. Fiji: an open-source platform for biological-image analysis. *Nat Methods.* 2012;9(7):676-682.

25. Jones ND, Turvey SE, Van Maurik A, et al. Differential susceptibility of heart, skin, and islet allografts to T cell-mediated rejection. *J Immunol.* 2001;166(4):2824-2830.

26. He C, Heeger PS. CD8 T cells can reject major histocompatibility complex class I-deficient skin allografts. *Am J Transplant.* 2004;4(5):698-704.

27. Maltzman JS, Turka LA. Conditional gene expression: a new tool for the transplantologist. *Am J Transplant.* 2007;7(4):733-740.

28. Feil S, Valtcheva N, Feil R. Inducible Cre mice. *Methods Mol. Biol.* 2009;530:323-363.

29. Fantini MC, Becker C, Monteleone G, Pallone F, Galle PR, Neurath MF. Cutting edge: TGF-β induces a regulatory phenotype in CD4 + CD25 – T cells through Foxp3 induction and down-regulation of Smad7. *J Immunol.* 2004;172(9):5149-5153.

30. Wan YY, Flavell RA. 'Yin-Yang' functions of TGF- β and Tregs in immune regulation. *Immunol Rev.* 2007;220(1):199-213.

31. Chanda S, Nandi S, Chawla-Sarkar M. Rotavirus-induced miR-142-5p elicits proviral milieu by targeting non-canonical transforming growth factor beta signalling and apoptosis in cells. *Cell Microbiol.* 2016;18(5):733-747.

32. Gottwein E, Corcoran D, Mukherjee N, et al. Viral microRNA targetome of KSHV-infected primary effusion lymphoma cell lines. *Cell Host Microbe.* 2011;10(5):515-526.

33. Loeb G, Khan A, Canner D, et al. Transcriptome-wide miR-155 binding map reveals widespread noncanonical microRNA targeting. *Mol Cell.* 2012;48(5):760-770.

34. Nimmo R, Ciau-Uitz A, Ruiz-Herguido C, et al. MiR-142-3p controls the specification of definitive hemangioblasts during ontogeny. *Dev Cell.* 2013;26(3):237-249.

35. Talebi F, Ghorbani S, Chan WF, et al. MicroRNA-142 regulates inflammation and T cell differentiation in an animal model of multiple sclerosis. *J Neuroinflammation.* 2017;14(1):55.

36. Xu S, Wei J, Wang F, et al. Effect of miR-142-3p on the M2 macrophage and therapeutic efficacy against murine glioblastoma. *J Natl Cancer Inst.* 2014;106(8):1-11.

37. Kramer NJ, Wang WL, Reyes EY, et al. Altered lymphopoiesis and immunodeficiency in *miR-142* null mice. *Blood.* 2015;125:3720-3730.

38. Mildner A, Chapnik E, Varol D, et al. MicroRNA-142 controls thymocyte proliferation. *Eur J Immunol.* 2017;47(7):1142-1152.

39. Shelton MW, Walp LA, Basler JT, et al. Mediation of skin allograft rejection in scid mice by CD4+ and CD8+ T cells. *Transplantation.* 1992;54:278-286.

40. Vu MD, Amanullah F, Li Y, Demirci G, Sayegh MH, Li XC. Different costimulatory and growth factor requirements for CD4+ and CD8+ T cell-mediated rejection. *J Immunol.* 2004;173:214-221.

41. Nozaki T, Rosenblum JM, Ishii D, et al. CD4 T cell-mediated rejection of cardiac allografts in B cell deficient mice. *J Immunol.* 2008;181(8):5257-5263.

42. Kroemer A, Xiao X, Degauque N, et al. The innate NK cells, allograft rejection, and a key role for IL-15. *Am J Transplant.* 2008;180:7818-7826.

43. Epstein MM, Di Rosa F, Jankovis D, Sher A, Matzinger P. Successful T cell priming in B Cell deificient mice. *J Exp Med.* 1995;182:915-922.

44. He C, Schenk S, Zhang Q, et al. Effects of T cell frequency and graft size on transplant outcome in mice. *J Immunol.* 2004;172(1):240-247.

45. London CA, Lodge MP, Abbas AK. Functional responses and costimulatory dependence of memory CD4+ T cells. *J Immunol.* 1994;152:2675-2685.

46. Croft M, Bradley LM, Swain SL. Naive versus memory CD4 T cell response to antigen. *J Immunol.* 1998;160:3236-3243.

47. Valujskikh A, Li XC. Frontiers in nephrology: T cell memory as a barrier to transplant tolerance. *J Am Soc Nephrol.* 2007;18:2252-2261.

48. Pearl JP, Parris J, Hale DA, et al. Immunocopetent T-cells with memory-like phenotype are the dominant cell type following antibody mediated T-cell depletion. *Am J Transplant.* 2005;5:465-474.

49. Louis S, Braudeau C, Giral M, et al. Contrasting CD25hiCD4+T cells/FOXP3 patterns in chronic rejection and operational drug-free tolerance. *Transplantation.* 2006;81:398-407.

50. Gregori S, Casorati M, Amuchastegui S, Smiroldo S, Davalli A, Adorini L. Regulatory T cells induced by 1α,25-dihydroxyvitamin D$_3$ and mycophenolate mofetil treatment mediate transplantation tolerance. *J Immunol.* 2001;167:1945.

51. Thorstenson KM, Khoruts A. Generation of anergic and potentially immunoregulatory CD25$^+$CD4 T cells in vivo after induction of peripheral tolerance with intravenous or oral antigen. *J Immunol.* 2001;167:188.

52. Hara M, Kingsley CI, Niimi M, et al. IL-10 is required for regulatory T cells to mediate tolerance to alloantigens in vivo. *J Immunol.* 2001;166:3789.

53. Akl A, Jones ND, Rogers N, et al. An investigation to assess the potential of CD25highCD4+ T cells to regulate responses to donor alloantigens in clinically stable renal transplant recipients. *Transpl Int.* 2008;2:65-73.

54. Braudeau C, Racape M, Giral M, et al. Variation in numbers of CD4+CD25 high FOXP3+ T cells with normal immuno-regulatory properties in long-term graft outcome. *Transpl Int.* 2007;20:845-855.

55. Wei L, Wang M, Qu X, et al. Differential expression if microRNAs during allograft rejection. *Am J Transplant.* 2012;12(5):1113-1123.

56. Brouard S, Mansfield E, Braud C, et al. Identification of a peripheral blood transcriptional biomarker panel associated with operational renal allograft tolerance. *PNAS.* 2007;104(39):15448-15453.

57. Moraes-Viera PM, Takenaka MC, Silva HM, et al. GATA3 and dominant regulatory gene expression profile discriminate operational tolerance in human transplantation. *Clin Immunol.* 2012;142:117-126.

58. Daley SR, Jianbo M, Adams E, Cobbold SP, Waldmann H. A key role for TGFβ signaling to T cells in the long-term acceptance of allografts. *J Immunol.* 2007;179(6):3648-3654.

59. Cobbold SP, Castejon R, Adams E, et al. Induction of *foxP3*$^+$ regulatory T cells in the periphery of T cell receptor transgenic mice tolerized to transplant. *J Immunol.* 2004;172(10):6003-6010.

SUPPORTING INFORMATION

Additional supporting information may be found online in the Supporting Information section.